

Optically pumped polaritons in perovskite light-emitting diodes

Leng, Meiyang; Wu, Jinqi; Dini, Kevin; Liu, Jing; Hu, Zehua; Tang, Jiang; Liew, Timothy Chi Hin; Sun, Handong; Su, Rui; Xiong, Qihua

2023

Leng, M., Wu, J., Dini, K., Liu, J., Hu, Z., Tang, J., Liew, T. C. H., Sun, H., Su, R. & Xiong, Q. (2023). Optically pumped polaritons in perovskite light-emitting diodes. *ACS Photonics*, 10(5), 1349-1355. <https://dx.doi.org/10.1021/acsp Photonics.2c01999>

<https://hdl.handle.net/10356/168988>

<https://doi.org/10.1021/acsp Photonics.2c01999>

This document is the Accepted Manuscript version of a Published Work that appeared in final form in *ACS Photonics*, copyright © 2023 American Chemical Society, after peer review and technical editing by the publisher. To access the final edited and published work see <https://doi.org/10.1021/acsp Photonics.2c01999>.

Downloaded on 22 Jul 2024 13:03:12 SGT

Optical pumped polaritons in perovskite light emitting diodes

Meiying Leng¹, Jinqi Wu¹, Kevin Dini¹, Jing Liu², Zehua Hu¹, Jiang Tang², Timothy C.H. Liew¹, Handong Sun¹, Rui Su^{1,3,*} and Qihua Xiong^{4,5,6,7,*}

¹Division of Physics and Applied Physics, School of Physical and Mathematical Sciences, Nanyang Technological University, Singapore 637371, Singapore

² School of Optical and Electronic Information, Huazhong University of Science and Technology, Wuhan, 430074, Hubei, P. R. China

³School of Electrical and Electronic Engineering, Nanyang Technological University, Singapore 637371, Singapore

⁴State Key Laboratory of Low-Dimensional Quantum Physics and Department of Physics, Tsinghua University, Beijing 100084, P.R. China.

⁵Frontier Science Center for Quantum Information, Beijing 100084, P.R. China

⁶Collaborative Innovation Center of Quantum Matter, Beijing, P.R. China

⁷Beijing Academy of Quantum Information Sciences, Beijing 100193, P.R. China

To whom the correspondence should be addressed. Emails: surui@ntu.edu.sg, and qihua_xiong@tsinghua.edu.cn

ABSTRACT

Lead halide perovskites have achieved significant progress in light-emitting diodes (LEDs) with high efficiency in the past decades. They are also ideal candidates for reaching the strong exciton–photon coupling regime, due to their large exciton binding energy and oscillator strength. The generation and control of exotic phenomena in perovskite electroluminescent microcavities, such as electrically pumped polariton lasing and polariton LEDs, operating in the strong coupling regime at room temperature, is still a great challenge. Here we demonstrate room temperature strong coupling in a perovskite LED structure. The best device shows a current efficiency of 4.5 cd/A and an external quantum efficiency of 1.4% while exhibiting anti-crossing behavior via optical pumping. Our approach represents a new strategy to explore the ultrafast LEDs as well as electrically pumped perovskite lasing.

Keywords: halide perovskites, strong light-matter coupling, exciton polariton, light emitting diodes

1. INTRODUCTION

In recent years, halide perovskites have drawn extensive attention due to their excellent properties, such as: large absorption coefficient (10^5 cm^{-1}),¹ high defect-tolerance,² bright emission throughout a broad wavelength range (about 410 - 850 nm),³ readily tuneable dimensionality and composition via ammonium institution (Methylammonium, Cs^+ , phenethyl ammonium),⁴ and stable excitons with large exciton binding energies at room temperature. Owing to these extraordinary properties, halide perovskites have exhibited great promise for typical optoelectronic applications, such as solar cells⁵, LEDs⁶⁻⁷, lasers⁸⁻¹³, etc. Currently, as a gain material, perovskite has shown decent performance. Amplified spontaneous emission and coherent lasing with extremely low threshold were achieved with perovskites in different morphologies and compositions in the past decade^{8-9, 14-17}. With strong oscillator strength and large exciton binding energy, halide perovskites also emerge as a promising platform for the strong light matter coupling regime, which allows to reach low threshold-polariton lasing at room temperature.¹⁸⁻²² Also, with long carrier diffusion length²³ and low defect density²⁴, LEDs based on halide perovskites has accomplished remarkable performance with an external quantum efficiency (EQE) over 25%⁶. Although significant progress has been made in lasers and light emitting devices with perovskite, the realization of an electrically pumped laser based on perovskites remains as a big challenge that has not be tackled yet.

Up to now, achieving an electrically pumped laser with perovskites generally has three main challenges: 1) the dilemma of high carrier mobility and large exciton binding energy, 2) optical losses from electrical contacts and electrical losses induced by polarons at high current densities, 3) strong ion migration in perovskite under biased operating conditions. Compared to conventional semiconductor lasers relying on stimulated emission of photons, polariton lasers, the coherent light source formed by polariton condensation, can work without electron population inversion.²⁵⁻²⁶ Thereby, they can outperform their weak-coupling counterparts with a much lower threshold density, and serve as better candidates for electrically pumped lasers with perovskites. Electrically pumped polariton lasers can be achieved by both LED device structures with P-N junctions²⁷ and nano devices structures²⁸ with tunneling effect. Compared to the nano devices, LEDs can be larger scaled, turning on with lower voltage at room temperature and showing better electroluminescence performance, which is better to achieve laser applications. However, one of the prerequisites is to achieve polaritons in perovskite LED structures. Polaritonic LEDs or electrically pumped polariton

lasing have been reported in traditional organic semiconductors²⁹ as well as in inorganic materials, such as GaAs, GaN and ZnO^{27,30}. Recently, electrically pumped polariton emission was achieved in a perovskite tunneling structure but limited to micrometer-sized perovskite crystals and working at cryogenic temperatures³¹. Until now, room-temperature polaritons in large-area perovskite LEDs has not achieved.

Here we report the realization of polaritons in perovskite LEDs via a vacuum deposition method at room temperature. Dual source thermal evaporation was utilized to achieve large-area perovskite thin films because of its good crystallinity, easily tuned composition, remarkable scalability and reproducibility. The resulting polariton LEDs showed electro-optical performances up to 1.4 % of external quantum efficiency and nearly 2000 cd/m² of luminance with a structure of ITO/PEDOT:PSS/ perovskite/B3PYMPM/LiF/Ag and an active area of 0.02 cm². As expected, polariton are observed as the CsBr/PbBr₂ molar ratio increased from 1.4–1.6 via optical pumping. Based on an optimal molar ratio of CsBr/PbBr₂, we then constructed the thermally evaporated perovskite LED structure with a large Rabi splitting of 42 meV. Moreover, we successfully varied the exciton photon detuning by changing the thickness of the organic layer. We believe our work represents an encouraging steppingstone to achieve electrically pumped perovskite lasing.

2. RESULTS AND DISCUSSION

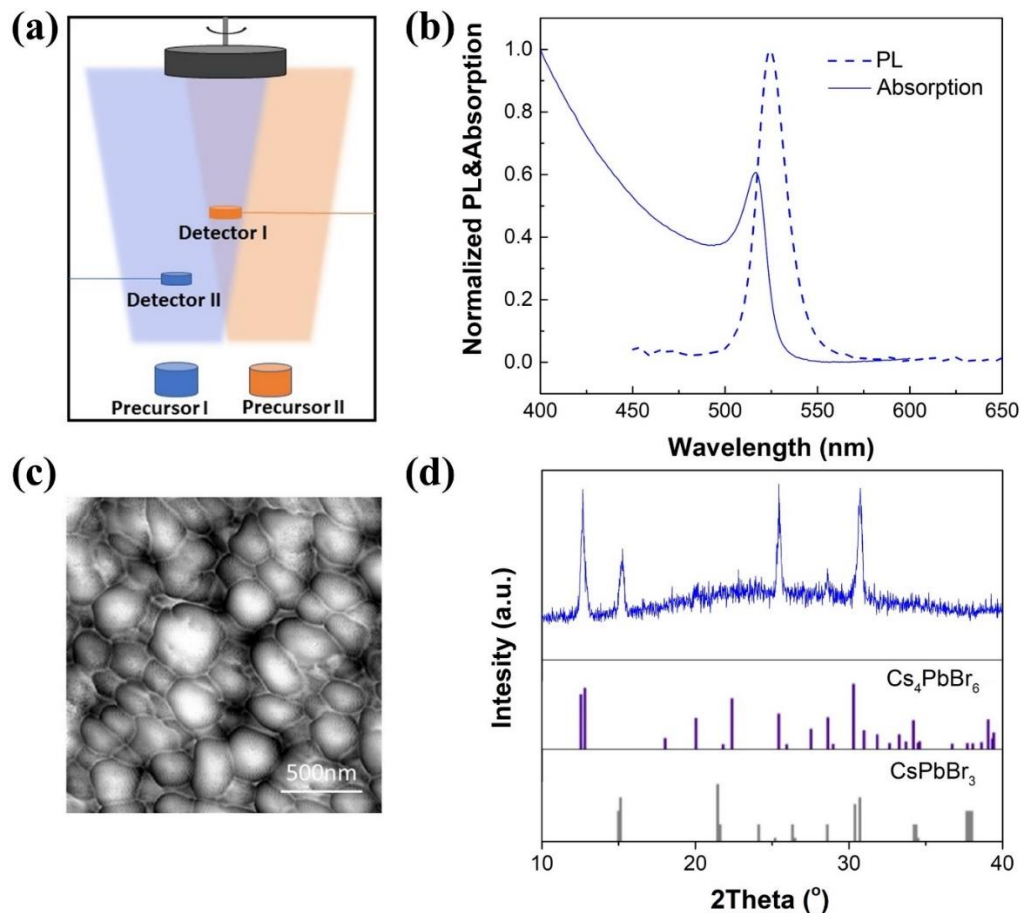


Figure 1. (a) Schematic demonstration of dual-source thermal evaporation. Typical perovskite thin film thin film made by dual-source thermal evaporation with Cs/Pb ratio as 1.6, temperature as 100 °C and evaporation rate as 1 Å/s (b) Photoluminescence (PL) and absorption spectra. (c) Atomic force microscopy (AFM) image. (d) X-ray diffraction pattern (XRD) and standard PDF card for Cs₄PbBr₆ and CsPbBr₃.

The preparation process of CsPbBr₃ thin films via dual-source co-evaporation of PbBr₂ and CsBr is illustrated in Figure. 1(a). Various Cs/Pb ratio and substrate temperature were tuned and their properties are shown in Figure. S1-3 and Table. S1. We chose a typical perovskite sample (Cs/Pb ratio: 1.6, substrate temperature: 100 °C, evaporation rate: 1 Å/s) to further study its characteristics. Absorption and fluorescence spectra of our perovskite thin film are shown in Figure. 1(b). The absorption spectrum shows that the exciton peak of perovskite thin film was around 517 nm. In

the photoluminescence (PL) spectrum, an emission peak at 524 nm with a full width at half maximum value of 18 nm can be observed. Compared to the sample made by solution method, the sample via vacuum method shows a stronger exciton peak.³²⁻³³ The photoluminescence quantum yield (PLQY) of this perovskite thin film is about 37%. (Figure. S4) Details of PLQY measurements are explained in supporting information. The atomic force microscopy (AFM) image of the perovskite film is shown in Figure. 1(c), which shows a surface roughness of around 6.98 nm with large grains. As shown in Figure. 1(d), X-ray diffraction (XRD) patterns reveal the phases of typical samples. The peaks near 12.7° are attributed to (012) and (110) planes of Cs₄PbBr₆, and that at 15.3° belongs to (110) plane of CsPbBr₃. The peak position is identical to that of mixed phases of CsPbBr₃ and Cs₄PbBr₆.

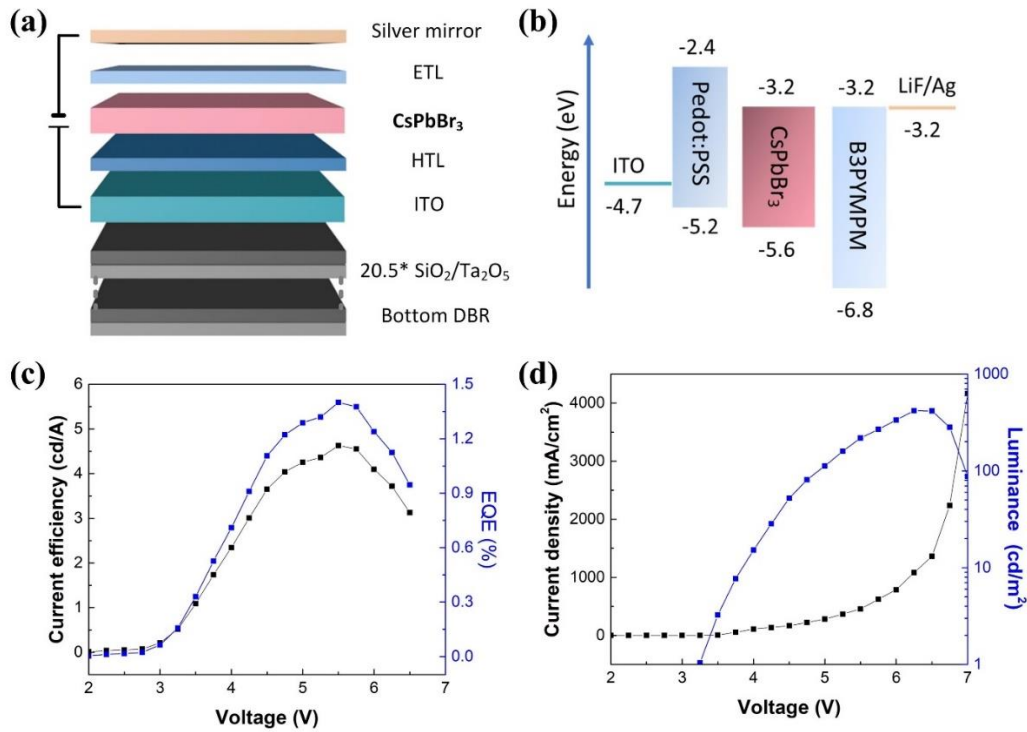


Figure 2. (a) Polariton LED structure configuration (b) Energy band diagram. (c) Current efficiency and external quantum efficiency (EQE) curves of a typical device. d) Current density–voltage (J–V) and luminance–voltage (L–V) curves of a typical device.

After determining the optical properties and phase of the perovskite film deposited by the vacuum co-evaporation, we further fabricated polariton LED devices based on the perovskite films. Considering for both device and cavities, the ideal structure for electrically pumped perovskite polariton laser or LED is shown in [Figure. 2\(a\)](#). The silver thin film was used both as top mirror and electrode. And the bottom mirror is distributed Bragg reflector (DBR) while the electrode is indium doped tin oxide (ITO). We further carried out transfer matrix calculations to determine the thicknesses for each layer, in order to achieve a proper cavity mode that can strongly couple to perovskite excitons. ([Figure. S5](#)) Here we chose the thickness of each layer (ITO, PEDOT:PSS, perovskite, B3PYMPM, LiF and Ag) as 80, 40, 110, 40, 1 and 50 nm, respectively. It is worth to note that the LiF layer was ignored in the simulation due to its rather thin thickness. The energy band diagram of our device (ITO/PEDOT:PSS/perovskite/B3PYMPM/LiF/Ag) is shown in [Figure. 2\(b\)](#). Please note that all devices including the ones fabricated by solution method studied in this paper employ this device structure.

The electroluminescent (EL) properties of devices were studied by using a Keithley 2400 source-meter and luminance & Colour Meter CS-200. (Devices Characterization Section, Supporting Information). The Cs/Pb ratio and evaporation rate were varied to explore better performance, which is shown in [Table. S2-3](#). The EQE peaked with the Cs/Pb ratio of 1.4:1, which may be due to the larger resistivity of Cs_4PbBr_6 .³⁴⁻³⁵ Choosing the Cs/Pb ratio as 1.4, temperature as 100 °C and evaporation rate as 1 Å/s, the champion device was successfully fabricated. It exhibits a turn on voltage of 2.8 V, a best EQE of 1.4% with a luminance near to 2000 cd/m^2 ([Figure. 2\(c,d\)](#)).

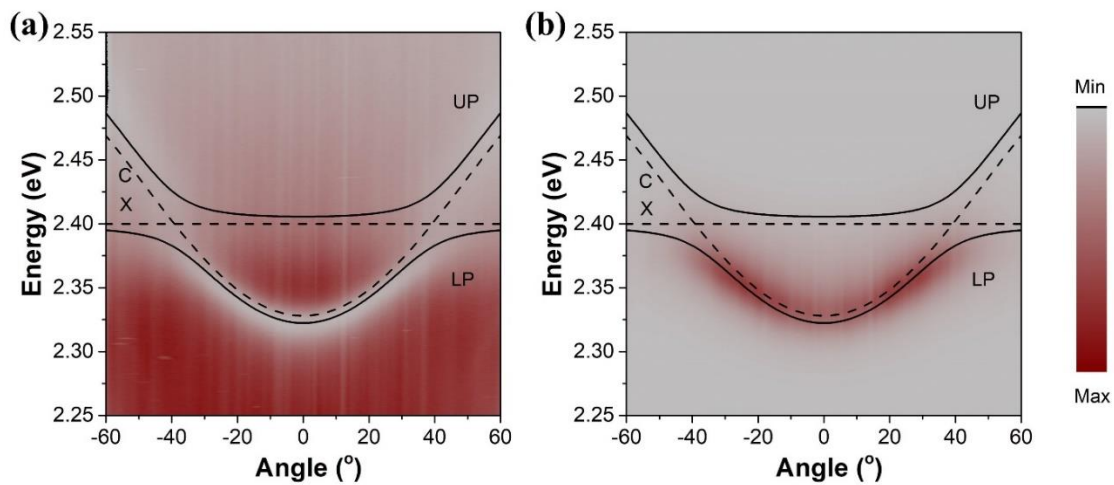


Figure 3. Polariton dispersion. (a) Angle-resolved white light reflectivity and (b) Angle resolved photoluminescence spectrum. The exciton energy (E_x) and the cavity photon dispersion E_c are shown as the dash lines and curves, respectively. The upper and lower polariton band are shown as solid curves, named UP and LP, respectively.

After verifying the device function, we characterized our device by angle-resolved white light reflectivity and photoluminescence (PL). Details of the setup for the k-space characterization are shown in the Methods, and all data shown in this paper are characterized at room temperature. It is worth to note that our LED device is very uniform, almost with the same spectrum while moving the test area. Parameters were also tuned to reach a balance for optoelectronic performance and strong coupling. (Figure. S6-8) With a Cs/Pb ratio as 1.6, temperature of 100 °C and evaporation rate of 1 Å/s, the LED device exhibited both clear optical pumped anti-crossing behavior and an EQE of 0.4%. Figure. 3a shows the angle-resolved reflection spectra from our typical perovskite device. It is important to note that a clear upper polariton branch was observed in the reflection spectra, which strongly suggests the strong coupling regime. To the best of our knowledge, this is the first time that the upper polariton branch was directly observed in CsPbBr₃ microcavities. We further observed the PL under non-resonant excitation (473 nm), exhibiting two resonant dips moving toward and away from the exciton mode with an anti-crossing angle dispersion, clearly corresponding to the lower (LP) and upper (UP) polariton modes generated from the exciton-photon coupling, as shown in Figure. 3b. The angular dispersion of the LP and UP modes anti-crossing at $\theta \sim 38^\circ$. We fitted the UP and LP dispersion curves with a two-mode coupled oscillator model,³⁶

$$E_{UP,LP}(\theta) = \frac{1}{2}(E_c(\theta) + E_x) \pm \frac{1}{2}\sqrt{(E_c(\theta) - E_x)^2 + (2g_0)^2}, \quad (1)$$

where E_x is the exciton energy, E_c is the cavity photon energy (dependent on the emission angle), $2g_0$ is Rabi splitting in this cavity system and the cavity detuning is defined by $\Delta = E_c(0) - E_x$. From the fitting, we extracted a Rabi splitting of 42 meV (solid lines) and cavity detuning of -72 meV (dashed lines). Compared to the Rabi splitting achieved in previous reports²³, the Rabi splitting in our LED structure is relatively smaller due to the presence of ITO and carrier transport layers,

which efficiently dissociate the perovskite excitons and reduce the effective exciton oscillator strength. In addition, the polycrystalline nature of our perovskite thin film would also reduce the Rabi splitting.

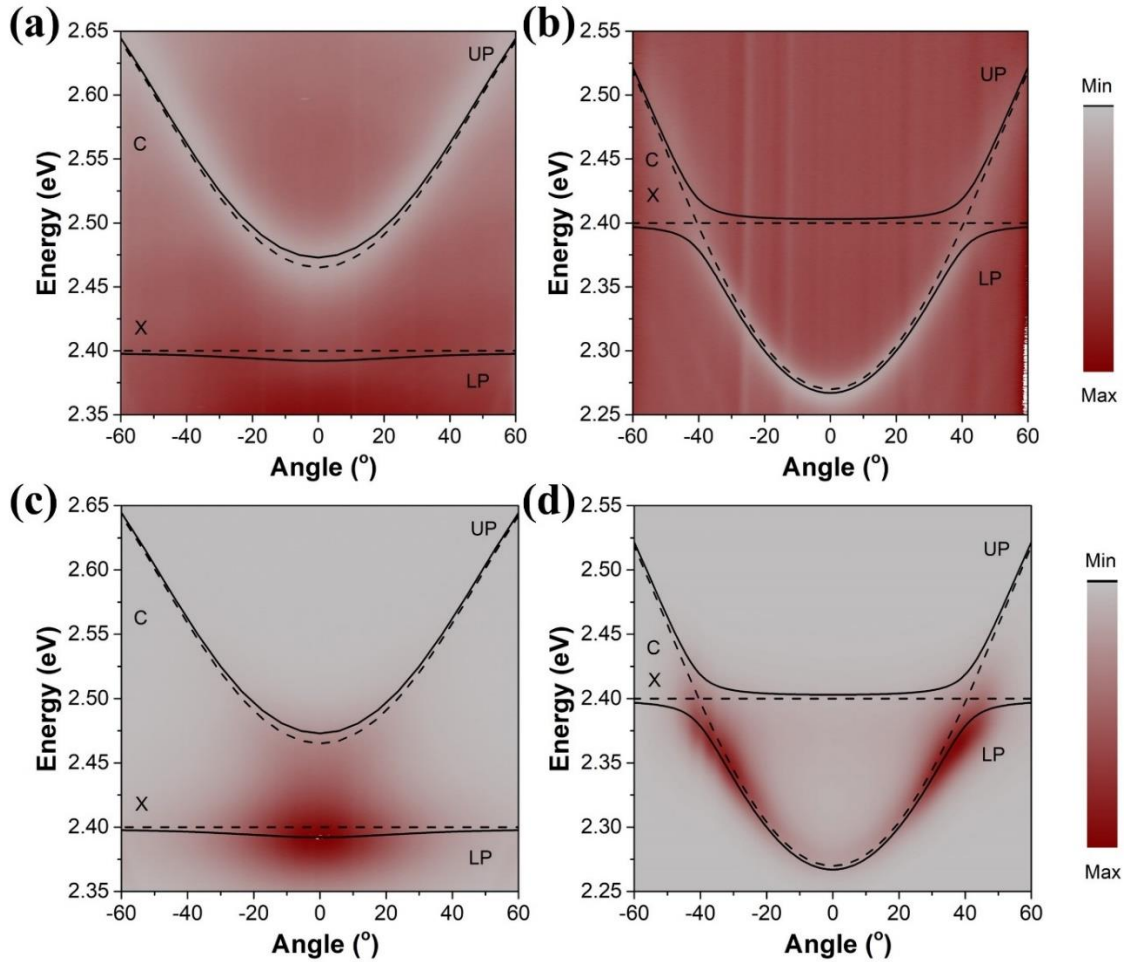


Figure 4. Cavity detuning variation. (a-b) Angle-resolved white light reflectivity and (c-d) Angle resolved photoluminescence spectrum for the device with a positive detuning (65 meV) or higher negative detuning (-130 meV), respectively.

Samples with different cavity detuning were fabricated by tuning the thickness of B3PYMPM. Figure 4(a-b) show the angle-resolved reflectivity spectra of polaritons with positive (65meV) and negative (-130 meV) detuning, respectively. Figure 4(c-d) are the corresponding angle-resolved photoluminescence spectra. The Rabi splitting of the device with positive (65 meV) and negative

detuning (-130 meV) are 48 meV and 45 meV, respectively. The device with higher negative detuning (-130 meV) demonstrates the presence of a relaxation bottleneck, which shows an emission maximum at a large angle. For this device, the emission maximum locates at 36° while the emission maximum of the control device locates at 0° . This bottleneck effect existing in the larger detuning sample is related to the inefficient polariton scattering to $k_{\parallel}=0$ owing to the slower polariton relaxation rate when the dispersion is steeper.³⁷ We further studied the stability of the device, particularly with the angle resolved photoluminescence. The storage stability has been studied, the sample with negative detuning (-130 meV) was placed at room temperature with a humidity of $\sim 60\%$. After seven days, the dispersion of the sample was almost the same (Figure S9).

For the purpose of comparison, we have also explored the solution method to prepare the perovskite thin film (refer to Methods section for more details). The device structure is the same with the polariton LED device prepared by vacuum co-evaporation method. The same phenomena are achieved in this device. The same batch of samples turned on at 6 V for the LED devices and the EL peak was located at 523 nm. (Figure. S10) Moreover, this device also shows a clear anti-crossing while measuring the angle resolved reflectivity. However, the solution-prepared devices showed rather smaller Q value deduced from the angle resolved photoluminescence spectroscopy. After the fitting, the exciton energy, cavity photon energy, Rabi splitting and detuning are 2.402 eV, 2.26 eV and 32 meV, respectively. The exciton energy is larger than the device made by vacuum method while the Rabi splitting is smaller.

3. CONCLUSION

To summarize, we have developed perovskite optical polariton devices with LED structure via vacuum method, which utilizes perovskite thin film as a gain medium and DBR integrated into ITO electrode and silver thin film as an optical cavity and electrode. These structures with polaritons can also operate as LEDs with a good “roll-off” behavior. Until now, the performance of perovskite LEDs fabricated by the vacuum method are not as high as the common LEDs made by solution method but support more precise control and tuning of the thickness of each layer in perovskite LEDs, which was more suitable for the generation of polaritons. We anticipate that electrically pumped exciton-polariton condensation could be achieved while the EQE of the vacuum made perovskite LEDs improved. All in all, our results prove the feasibility of polaritons

in the perovskite with electrical injection and further demonstrate a practical architecture for implementing a perovskite-based laser diode device.

4. METHODS

Device fabrication. The DBR was grown on a silicon substrate by E-beam evaporation. It consisted of 20.5 periods of alternate layers of SiO_2 (87.5 nm) and Ta_2O_5 (60.2 nm). Indium tin oxide (ITO) layer (80 nm) was then deposited by magnetron sputtering. After the sputtering, it subsequently treated with UV-Ozone at 50 °C for 15 min before using. As for the PEDOT:PSS layer, the PEDOT:PSS was spin-coated at 4000 rpm for 60 s and was baked at 150 °C for 20 min. The perovskite layers were made by two methods. For the vacuum method, perovskite thin film is formed by dual source evaporation of CsBr and PbBr_2 in separate crucibles. As for the solution method, perovskite thin film was made by spin coating using a CsPbBr_3 /PEO mixed DMF solution. After the spin coating, it will anneal on the hot plate at 80 °C for 15 min. The electron injection layers (B3PYMPM, also as hole blocking layers) with different thicknesses were deposited by evaporation. Finally, LiF (1 nm) and Ag (50 nm) were deposited sequentially.

Optical measurements. The absorption spectrum was measured by the commercial micro-transmission/absorption spectrometer (Craic 20/20). The steady-state PL spectra were measured by a confocal microscopic spectrometer (LabRAM HR800, Horiba) at room temperature using a helium cadmium laser (325 nm) as a pump source. Angle-resolved spectra were recorded using a homemade spectroscopy set-up that comprised white light (reflectivity) and a 473 nm laser (PL). The spectra were measured through a high numerical aperture ($NA = 0.9$) 100× microscope objective, covering an angular range of $\pm 64^\circ$. The light emission was collected and sent to a Horiba550 with a 1024×256 pixels liquid nitrogen cooled charge coupled device (CCD) and a 600 lines/mm grating.

EL measurements. The electroluminescent (EL) properties of devices were studied by using Keithley 2400 source meter and CS-200 color and luminance meter. The device performance parameters (EQE, current efficiency, etc.) could be automatically calculated by software via equation. Details are shown in supporting information.

ASSOCIATED CONTENT

Supporting Information Available: parameters in thermal evaporation, PLQY, simulation result, EL measurement, device tuning to balance rabi splitting and EQE, Air stability of perovskite polariton LED devices, device via solution method. This material is available free of charge via the Internet at <http://pubs.acs.org>.

AUTHOR INFORMATION

Corresponding Author

*Email: qihua_xiong@tsinghua.edu.cn, and surui@ntu.edu.sg

Author Contributions

Notes

The authors declare no competing financial interest.

FUNDING SOURCES

Q.X. gratefully acknowledges funding support from the National Natural Science Foundation of China (grant NO. 12020101003 and 92250301) and strong support from the State Key Laboratory of Low-Dimensional Quantum Physics at Tsinghua University. R.S. would like to thank the funding support from Nanyang Technological University via a Start-Up Grant Scheme and the Singapore Ministry of Education via the AcRF Tier 3 Programme “Geometrical Quantum Materials”(MOE2018-T3-1-002).

REFERENCES

1. Yin, W. J.; Shi, T.; Yan, Y., Unique properties of halide perovskites as possible origins of the superior solar cell performance. *Adv. Mater.* **2014**, *26*, 4653-8.
2. Yin, W. J.; Shi, T.; Yan, Y., Unusual defect physics in CH₃NH₃PbI₃ perovskite solar cell absorber. *Appl. Phys. Lett.* **2014**, *104*, 063903.
3. Worku, M.; Tian, Y.; Zhou, C.; Lin, H.; Chaaban, M.; Xu, L.-J.; He, Q.; Beery, D.; Zhou, Y.; Lin, X.; Su, Y.-F.; Xin, Y.; Ma, B., Hollow metal halide perovskite nanocrystals with efficient blue emissions. *Sci. Adv.* **2020**, *6*, 5961.
4. Saidaminov, M. I.; Mohammed, O. F.; Bakr, O. M., Low-dimensional-networked metal halide perovskites: The next big thing. *ACS Energy Lett.* **2017**, *2*, 889-896.
5. Li, X.; Z., W.; Guo, X.; Lu, C.; Wei, J.; Fang, J., Constructing heterojunctions by surface sulfidation for efficient inverted perovskite solar cells. *Science* **2022**, *375*, 434-437.
6. Ma, D.; Lin, K.; Dong, Y.; Choubisa, H.; Proppe, A. H.; Wu, D.; Wang, Y. K.; Chen, B.; Li, P.; Fan, J. Z.; Yuan, F.; Johnston, A.; Liu, Y.; Kang, Y.; Lu, Z. H.; Wei, Z.; Sargent, E. H., Distribution control enables efficient reduced-dimensional perovskite LEDs. *Nature* **2021**, *599*, 594-598.
7. Yu, S.; Hu, J.; Zhang, H.; Zhao, G.; Li, B.; Xia, Y.; Chen, Y., Recent progress in AC-driven organic and perovskite electroluminescent devices. *ACS Photonics* **2022**, *9*, 1852–1874.
8. Xing, G.; Mathews, N.; Lim, S. S.; Yantara, N.; Liu, X.; Sabba, D.; Gratzel, M.; Mhaisalkar, S.; Sum, T. C., Low-temperature solution-processed wavelength-tunable perovskites for lasing. *Nat. Mater.* **2014**, *13*, 476-80.
9. Zhang, Q.; Ha, S. T.; Liu, X.; Sum, T. C.; Xiong, Q., Room-temperature near-infrared high-Q perovskite whispering-gallery planar nanolasers. *Nano Lett.* **2014**, *14*, 5995-6001.
10. Zhu, H.; Fu, Y.; Meng, F.; Wu, X.; Gong, Z.; Ding, Q.; Gustafsson, M. V.; Trinh, M. T.; Jin, S.; Zhu, X. Y., Lead halide perovskite nanowire lasers with low lasing thresholds and high quality factors. *Nat. Mater.* **2015**, *14*, 636-42.
11. Zhang, Q.; Su, R.; Liu, X.; Xing, J.; Sum, T. C.; Xiong, Q., High-quality whispering-gallery-mode lasing from cesium lead halide perovskite nanoplatelets. *Adv. Funct. Mater.* **2016**, *26*, 6238-6245.
12. Jia, Y.; Kerner, R. A.; Grede, A. J.; Rand, B. P.; Giebink, N. C., Continuous-wave lasing in an organic–inorganic lead halide perovskite semiconductor. *Nat. Photonics* **2017**, *11*, 784-788.
13. Zhang, Q.; Shang, Q.; Su, R.; Do, T. T. H.; Xiong, Q., Halide perovskite semiconductor lasers: materials, cavity design, and low threshold. *Nano Lett.* **2021**, *21*, 1903-1914.
14. Deschler, F.; Price, M.; Pathak, S.; Klintberg, L. E.; Jarausch, D. D.; Higler, R.; Huttner, S.; Leijtens, T.; Stranks, S. D.; Snaith, H. J.; Atature, M.; Phillips, R. T.; Friend, R. H., High photoluminescence efficiency and optically pumped lasing in solution-processed mixed halide perovskite semiconductors. *J. Phys. Chem. Lett.* **2014**, *5*, 1421-6.
15. Wang, Y.; Li, X.; Song, J.; Xiao, L.; Zeng, H.; Sun, H., All-Inorganic Colloidal Perovskite Quantum Dots: A New Class of Lasing Materials with Favorable Characteristics. *Adv. Mater.* **2015**, *27*, 7101-8.

16. Fu, Y.; Zhu, H.; Schrader, A. W.; Liang, D.; Ding, Q.; Joshi, P.; Hwang, L.; Zhu, X. Y.; Jin, S., Nanowire lasers of formamidinium lead halide perovskites and their stabilized alloys with improved stability. *Nano. Lett.* **2016**, *16*, 1000-8.
17. Roh, K.; Zhao, L.; Gunnarsson, W. B.; Xiao, Z.; Jia, Y.; Giebink, N. C.; Rand, B. P., Widely tunable, room temperature, single-mode lasing operation from mixed-halide perovskite thin films. *ACS Photonics*, **2019**, *6*, 3331–3337.
18. Su, R.; Diederichs, C.; Wang, J.; Liew, T. C. H.; Zhao, J.; Liu, S.; Xu, W.; Chen, Z.; Xiong, Q., Room-temperature polariton lasing in all-inorganic perovskite nanoplatelets. *Nano Lett.* **2017**, *17*, 3982-3988.
19. Su, R.; Wang, J.; Zhao, J.; Xing, J.; Zhao, W.; Diederichs, C.; Liew, T. C. H.; Xiong, Q., Room temperature long-range coherent exciton polariton condensate flow in lead halide perovskites. *Sci. Adv.* **2018**, *4*, 0244.
20. Su, R.; Ghosh, S.; Wang, J.; Liu, S.; Diederichs, C.; Liew, T. C. H.; Xiong, Q., Observation of exciton polariton condensation in a perovskite lattice at room temperature. *Nat. Phys.* **2020**, *16*, 301-306.
21. Wu, J.; Ghosh, S.; Su, R.; Fieramosca, A.; Liew, T. C. H.; Xiong, Q., Nonlinear parametric scattering of exciton polaritons in perovskite microcavities. *Nano Lett.* **2021**, 3120-3126.
22. Ghosh, S.; Su, R.; Zhao, J.; Fieramosca, A.; Wu, J.; Li, T.; Zhang, Q.; Li, F.; Chen, Z.; Liew, T. C. H.; Sanvitto, D.; Xiong, Q., Microcavity exciton polaritons at room temperature. *Photonics Insights*. **2022**, *1*, R04.
23. Stranks, S. D.; Eperon, G. E.; Grancini, G.; Menelaou, C.; Alcocer, M. J. P.; Leijtens, T.; Herz, L. M.; Petrozza, A.; Snaith, H. J., Electron-hole diffusion lengths exceeding 1 micrometer in an organometal trihalide perovskite absorber. *Science* **2013**, *342*, 341–344.
24. Kang, J.; Wang, L. W., High defect tolerance in lead halide perovskite CsPbBr₃. *J. Phys. Chem. Lett.* **2017**, *8*, 489-493.
25. Kim, S.; Zhang, B.; Wang, Z.; Fischer, J.; Brodbeck, S.; Kamp, M.; Schneider, C.; Höfling, S.; Deng, H., Coherent polariton laser. *Phys. Rev. X* **2016**, *6*, 011026.
26. Deng, H.; Weihs, G.; Snoke, D.; Bloch, J.; Yamamoto, Y., Polariton lasing vs. photon lasing in a semiconductor microcavity. *Proc. Nat. Acad. Sci.* **2003**, *100*, 15318–15323.
27. Schneider, C.; Rahimi-Iman, A.; Kim, N. Y.; Fischer, J.; Savenko, I. G.; Amthor, M.; Lermer, M.; Wolf, A.; Worschech, L.; Kulakovskii, V. D.; Shelykh, I. A.; Kamp, M.; Reitzenstein, S.; Forchel, A.; Yamamoto, Y.; Hofling, S., An electrically pumped polariton laser. *Nature* **2013**, *497*, 348-52.
28. Graf, A.; Held, M.; Zakharko, Y.; Tropsch, L.; Gather, M. C.; Zaumseil, J., Electrical pumping and tuning of exciton-polaritons in carbon nanotube microcavities. *Nature Mater.* **2017**, *16*, 911–917.
29. Chang, J. F.; Lin, T. Y.; Hsu, C. F.; Chen, S. Y.; Hong, S. Y.; Ciou, G. S.; Jaing, C. C.; Lee, C. C., Development of a highly efficient, strongly coupled organic light-emitting diode based on intracavity pumping architecture. *Opt. Express* **2020**, *28*, 39781-39789.
30. Gu, J.; Chakraborty, B.; Khatoniar, M.; Menon, V. M., A room-temperature polariton light-

emitting diode based on monolayer WS₂. *Nat. Nanotechnol.* **2019**, *14*, 1024-1028.

31. Wang, T.; Zang, Z.; Gao, Y.; Lyu, C.; Gu, P.; Yao, Y.; Peng, K.; Watanabe, K.; Taniguchi, T.; Liu, X.; Gao, Y.; Bao, W.; Ye, Y., Electrically pumped polarized exciton-polaritons in a halide perovskite microcavity. *Nano Lett.* **2022**, *22*, 5175–5181.

32. Li, C.; Zang, Z.; Han, C.; Hu, Z.; Tang, X.; Du, J.; Leng, Y.; Sun, K., Highly compact CsPbBr₃ perovskite thin films decorated by ZnO nanoparticles for enhanced random lasing. *Nano Energy* **2017**, *40*, 195-202.

33. Lin, K.; Xing, J.; Quan, L. N.; de Arquer, F. P. G.; Gong, X.; Lu, J.; Xie, L.; Zhao, W.; Zhang, D.; Yan, C.; Li, W.; Liu, X.; Lu, Y.; Kirman, J.; Sargent, E. H.; Xiong, Q.; Wei, Z., Perovskite light-emitting diodes with external quantum efficiency exceeding 20 percent. *Nature* **2018**, *562*, 245-248.

34. Yuan, Y.; Yao, Q.; Zhang, J.; Wang, K.; Zhang, W.; Zhou, T.; Sun, H.; Ding, J., Negative photoconductivity in Cs₄PbBr₆ single crystal. *Phys. Chem. Chem. Phys.* **2020**, *22*, 14276-14283.

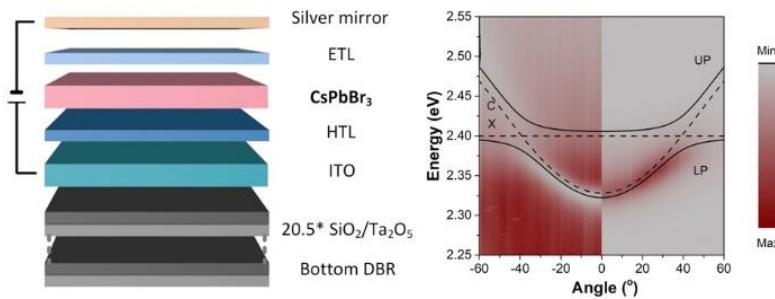
35. Cha, J. H.; Han, J. H.; Yin, W.; Park, C.; Park, Y.; Ahn, T. K.; Cho, J. H.; Jung, D. Y., Photoresponse of CsPbBr₃ and Cs₄PbBr₆ perovskite single crystals. *J. Phys. Chem. Lett.* **2017**, *8*, 565-570.

36. Deng, H.; Haug, H.; Yamamoto, Y., Exciton-polariton Bose-Einstein condensation. *Rev. Mod. Phys.* **2010**, *82*, 1489-1537.

37. Tassone, F.; Piermarocchi, C.; Savona, V.; Quattropani, A.; Schwendimann, P., Bottleneck effects in the relaxation and photoluminescence of microcavity polaritons. *Phys. Rev. B* **1997**, *56*, 7554.

Optical pumped polaritons in perovskite light emitting diodes

Meiying Leng, Jinqi Wu, Kevin Dini, Jing Liu, Zehua Hu, Jiang Tang, Timothy C.H. Liew, Handong Sun, Rui Su* and Qihua Xiong*



Brief synopsis: The workable perovskite light emitting diode made in vacuum method, combined with tunable anti-crossing behavior at room temperature, proves the feasibility of polariton in the perovskite with electrical injection and further demonstrates a practical architecture for implementing a perovskite-based laser diode device.